Distributed Perimeter Flow Control of Transport Networks

Ruzanna Mat Jusoh
PhD student
School of Engineering
University of Glasgow

Dr Konstantinos Ampountolas
Lecturer in Transportation Engineering
School of Engineering
University of Glasgow

Abstract

In this paper, we develop a distributed control scheme for the perimeter traffic flow control problem in urban road networks. The proposed scheme determines optimally distributed input flows for a number of gates located at the periphery of a protected network area. A parsimonious model is employed to describe the traffic dynamics of the protected network. To describe traffic dynamics outside of the protected area, we augment the basic state-space model with additional state variables for the queues at store-and-forward origin links at the periphery. We aim to equalise the relative queues at origin links and maintain the vehicle accumulation in the protected network around a desired point, while the system's throughput is maximised. The perimeter traffic flow control problem is formulated as a convex optimal control problem with constrained control and state variables. Simulation results are carried for a protected area of downtown San Francisco with fifteen gates of different geometric characteristics. Results demonstrate the efficiency and equity properties of the proposed approach to better manage excessive queues outside of the protected area and optimally distribute the input flows.

1 Introduction

Traffic congestion on urban road networks is deemed to inefficient road operations and excessive traffic demand, which calls for drastic solutions. The performance of road infrastructure is usually assessed by microscopic models at the link and/or junction level. In an attempt to assess the performance of urban road networks at a macroscopic level, a parsimonious but not accurate model is often used. It primarily shows the relationship between average network flow and vehicle accumulation or density. A macroscopic model of steady-state urban traffic was proposed by Godfrey (1969); Herman and Prigogine (1979), further developed by Ardekani and Herman (1987); Daganzo (2007); Daganzo and Geroliminis (2008); Farhi et al. (2011) and fitted to experimental data by Mahmassani et al. (1987); Geroliminis and Daganzo (2008); Ampountolas and Kouvelas (2015) and others. This model is the so-called Macroscopic or Network Fundamental Diagram (MFD or NFD) of urban road networks; it presumes (under certain regularity conditions) that traffic flows dynamics can be treated macroscopically as a single-region dynamic system with vehicle accumulation n (or density) as a state variable. The main feature of the NFD (with a concave like-shape as in Fig. 1) is that for a critical vehicle accumulation $\hat{n}$ flow capacity is reached (maximum throughput). This property can be utilised to introduce perimeter flow control policies to improve mobility in single-region homogeneous (Daganzo, 2007; Keyvan-Ekbatani et al., 2012) or multi-region heterogeneous networks (Geroliminis et al., 2013; Aboudolas and Geroliminis, 2013) and others. For an updated review of this vast area of research the interested reader is referred to Haddad (2015). A perimeter flow control policy "meters" the input flow to the system and hold vehicles outside a protected area if necessary, so as to maximise the throughput.

Except of a few works such as Csikós et al. (2015), studies on the perimeter flow control assume that a single input flow ordered by a perimeter control strategy should be equally distributed to a number of candidate junctions at the periphery of the network, i.e., without

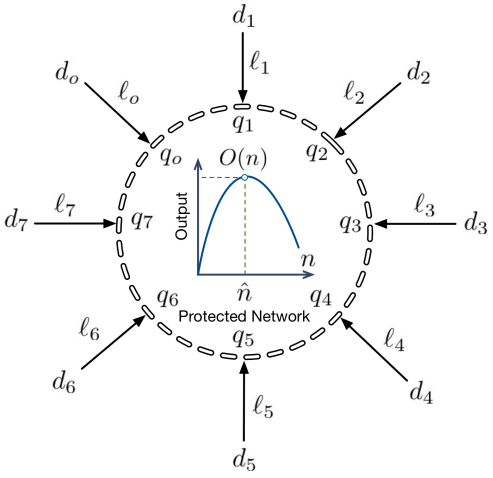

Figure 1: Protected network with entrance link dynamics.

taking into account the different geometric characteristics of origin links. Such a distribution policy applied independently to multiple gates of a protected network area would be efficient in case of unconstrained origin link queues for vehicle storage (i.e., infinite storage capacity). However, gated queues at origin links must be restricted to avoid interference with adjacent street traffic outside of the protected network area and geometric characteristics of the different gates must be taken into account in the optimisation. Thus, limited origin links storage capacity and the requirement of equity for drivers using different gates to enter a protected area are the main reasons towards distributed perimeter flow control.

In this work, we propose an integrated model for the distributed perimeter traffic flow control problem in urban road networks. We employ the renowned network or macroscopic fundamental diagram of urban networks to describe the traffic dynamics of the protected network area. To describe traffic dynamics outside of the protected area, we augment the basic state-space model with additional state variables for the queues at store-and-forward origin links at the periphery. The integrated model is then used to formulate a convenient convex or nonlinear optimal control problem with constrained control and state variables for distributed perimeter flow control. This scheme determines optimally distributed input flow values (or feasible entrance link green times) to avoid queues and delays at the perimeter of a protected area while system's output is maximised. We present preliminary results to demonstrate its efficiency and equity properties to better manage excessive queues outside of the protected network area and optimally distribute the input flows.

2 Perimeter Flow Modelling with Entrance Links Dynamics

Consider a protected network area with a number of controlled gates $o \in \mathcal{O} = \{1, 2, \ldots\}$ located at its periphery as shown in Fig. 1. The set $\mathcal{O}$ includes all the origin links whose outflow is essentially entering into the protected network from a number of controlled gates/entrances (e.g. signalised junctions or toll stations). In principle, the origin links at the periphery of the protected network would have different geometric characteristics, i.e., length, number of lanes, capacity, and saturation flows. The protected network traffic can be treated macroscopically as a single-region dynamic system with vehicle accumulation $n(t)$, $t \geq 0$ as a single state variable (Daganzo, 2007). To this end, assume there exists a well-defined function $O(n(t))$ (veh/h) that provides the estimated rate flow (output) at which vehicles complete trips per unit time either because they finish their trip within the network or because they move outside of the network. The output can be expressed as $O(n(t)) = (l/L)O_c(n(t))$, where L (m) is the average trip length in the network, l (m) is the average link length, and O_c (veh/h) is the total network circulating flow. In general, the circulating flow O_c can be estimated by the generalised definition of flow if $n(t)$ is observed in real-time.

Let $q_o(t)$ (veh/h) be the outflow of gate $o \in \mathcal{O}$ at time t. Also, let $q_{\text{out}}(t)$ (veh/h) and $d_n(t)$ (veh/h) be the total outflow and the uncontrolled traffic demand (disturbances) of the protected network at time t, respectively. The dynamics of the system are governed by the following nonlinear conservation equation

$$\dot{n}(t) = \sum_{o=1}^{|\mathcal{O}|} q_o(t) - q_{\text{out}}(t) + d_n(t), \tag{1}$$

where $q_{\text{out}}(t)$ is in general a nonlinear function of vehicle accumulation $n(t)$. Since the system evolves slowly with time t, we may assume that outflow $q_{\text{out}}(t) \propto O_c(n(t)$, and it may thus be given in terms of the output $O(n(t))$. Note that $q_o(t)$, $o \in \mathcal{O}$ are the input variables of the controlled gates/entrances, to be calculated by a distributed perimeter flow control strategy.

To describe traffic dynamics outside of the protected area, we augment the basic state-space model (1) with additional state variables for the queues at store-and-forward entrance links at the periphery. Each origin link ℓ_o receives traffic demand d_o and forward it into the protected network, as shown in Fig. 1. The queuing model for the entrance link dynamics is described by the following conservation equation

$$\dot{\ell_o}(t) = d_o(t) - q_o(t), \quad o \in \mathcal{O} = \{1, 2, \ldots\} \tag{2}$$

where $\ell_o(t)$ (veh) and $d_o(t)$ (veh/h) are the vehicle queue and traffic demand in origin link o at time t, respectively. The integrated model (1)–(2) can be extended to consider a broader class of state and control constraints as follows:

$$\begin{aligned} &0 \le n(t) \le n_{\max} \\ &0 \le \ell_o(t) \le \ell_{o,\max}, \quad o \in \mathcal{O} = \{1, 2, \ldots\} \\ &q_{o,\min} \le q_o(t) \le q_{o,\max}, \quad o \in \mathcal{O} = \{1, 2, \ldots\} \end{aligned} \tag{3}$$

where $n_{\max}$ is the maximum vehicle accumulation of the protected network; $\ell_{o,\max}$ is the maximum permissible capacity of link $o \in \mathcal{O}$; $q_{o,\min}$, $q_{o,\max}$ are the minimum and maximum permissible outflows, respectively; and, $q_{o,\min} > 0$ to avoid long queues and delays at the periphery of the network. Link capacities and maximum vehicle accumulation depend on geometric characteristics of the origin links (length, number of lanes) and the topology of the protected network, respectively. Minimum and maximum permissible outflows can easily be determined given saturation flows, minimum and maximum green times, and cycle times of a nominal traffic signal plan (or corresponding toll ticket) at each controlled gate of the protected network.

The presented model can be viewed as a nonlinear process with input variables $\mathbf{u}^{\mathsf{T}} = \begin{bmatrix} q_1 & q_2 & \cdots & q_{|O|} \end{bmatrix}$, state variables $\mathbf{x}^{\mathsf{T}} = \begin{bmatrix} n & \ell_1 & \ell_2 & \cdots & \ell_{|O|} \end{bmatrix}$, and disturbances $\mathbf{d}^{\mathsf{T}} = \begin{bmatrix} d_n & d_1 & d_2 & \cdots & d_{|O|} \end{bmatrix}$. Then, the continuous-time nonlinear state system (1), (2) with constraints (3) for a protected network with controlled gates $o \in \mathcal{O}$, may be rewritten in compact vector form as

$$\dot{\mathbf{x}}(t) = \mathbf{f}\left[\mathbf{x}(t), \mathbf{u}(t), \mathbf{d}(t), t\right], t \ge 0, \quad \mathbf{x}(0) = \mathbf{x}_0 \tag{4}$$

$$\mathbf{0} \le \mathbf{x}(t) \le \mathbf{x}_{\max} \tag{5}$$

$$\mathbf{u}_{\min} \le \mathbf{u}(t) \le \mathbf{u}_{\max} \tag{6}$$

where $\mathbf{f}$ is a nonlinear vector function reflecting the right-hand side of (1)–(2); $\mathbf{x}_0$ is a known initial state; and $\mathbf{x}_{\max}$, $\mathbf{u}_{\min}$, $\mathbf{u}_{\max}$ are vectors of appropriate dimension reflecting the upper and lower bounds of constraints (3).

Assuming a nonlinear representation of $q_{\text{out}}(t) \triangleq O(n(t))$, the continuous-time nonlinear model (4) may be linearised around some set point $\hat{\mathbf{s}}^{\mathsf{T}} = \begin{bmatrix} \hat{\mathbf{x}} & \hat{\mathbf{u}} & \hat{\mathbf{d}} \end{bmatrix}$, and directly translated into discrete-time, using Euler first-order time discretisation with sample time T, as follows

$$\Delta\mathbf{x}(k+1) = \mathbf{A}\Delta\mathbf{x}(k) + \mathbf{B}\Delta\mathbf{u}(k) + \mathbf{C}\Delta\mathbf{d}(k) \tag{7}$$

where $k = 0, 1, \ldots, N_o - 1$ is a discrete time index with optimisation horizon N_o; $\Delta(\cdot) \triangleq (\cdot) - \hat{\cdot}$ for all vectors; and $\mathbf{A} = \partial\mathbf{f}/\partial\mathbf{x}|_{\hat{\mathbf{s}}}$, $\mathbf{B} = \partial\mathbf{f}/\partial\mathbf{u}|_{\hat{\mathbf{s}}}$, $\mathbf{C} = \partial\mathbf{f}/\partial\mathbf{d}|_{\hat{\mathbf{s}}}$ are the state, control, and disturbance matrices, respectively. This discrete-time linear model is completely controllable and reachable, and will be used as a basis for control design. The sample time interval T is literally selected to be a common multiple of cycle lengths of all controlled gates at the periphery of the protected network, while $T \in [3, 5]$ minutes is usually appropriate for constructing a well-defined outflow function $O(n(t))$, given experimental data.

3 Distributed Perimeter Flow Control

A suitable control objective for a protected network area with origin links queue dynamics aims at: (a) equalising the relative vehicle queues $\ell_o/\ell_{o,\max}$, $o \in \mathcal{O}$ over time, and (b) maintaining the vehicle accumulation in the protected network around a set (desired) point $\hat{n}$ while the system's throughput is maximised. A quadratic criterion that considers this control objective has the form

$$J = \frac{1}{2} \sum_{k=0}^{N_o-1} \Big(\|\Delta\mathbf{x}(k)\|^2_{\mathbf{Q}} + \|\Delta\mathbf{u}(k)\|^2_{\mathbf{R}} \Big) \tag{8}$$

where $\mathbf{Q}$ and $\mathbf{R}$ are positive semi-definite and positive definite diagonal weighting matrices, respectively. The diagonal elements of $\mathbf{Q}$ are responsible for balancing the relative vehicle accumulation of the protected network $n/n_{\max}$ and the relative vehicle queues $\ell_o/\ell_{o,\max}$, $o \in \mathcal{O}$. Given that vehicle storage in the protected network is significantly higher than in the origin links, a meticulous selection of diagonal elements is required. A practicable choice is to set $\mathbf{Q} = \mathrm{diag}(1/w, 1/\ell_{1,\max}, \ldots, 1/\ell_{|\mathcal{O}|,\max})$, where the scale of $w \ll n_{\max}$ is of the order of $\sum_{o=1}^{|O|} \ell_{o,\max}$ to achieve equity. It becomes quite clear here that equity at origin links and efficiency of the protected network area are partially competitive criteria, hence a perimeter flow control strategy should be flexible enough to accommodate a particular trade-off (i.e. to give priority to the protected network or the outside area, e.g. to manage better excessive queues) to be decided by the responsible network authorities. Finally, the choice of the weighting matrix $\mathbf{R} \triangleq r\mathbf{I}$, $r > 0$ can influence the magnitude of the control actions and thus r should be selected via a trial-and-error process.

Rolling horizon control is a repetitive optimisation scheme, where at each time step an open-loop optimal control problem with finite horizon N_o and predicted demands $\mathbf{d}(k)$ is optimised, then only the first control move is applied to the plant and the procedure is carried out again. Given the known initial state $\mathbf{x}(0) = \mathbf{x}_0$, a static convex optimisation problem may be formulated over N_o due to the discrete-time nature of the involved process. To see this, assume $N_o = N_p$ and define the vectors

$$\begin{aligned}
\Delta\mathbf{X} &= \begin{bmatrix} \Delta\mathbf{x}(1)^\mathsf{T} & \Delta\mathbf{x}(2)^\mathsf{T} & \cdots & \Delta\mathbf{x}(N_o)^\mathsf{T} \end{bmatrix}^\mathsf{T} \\
\Delta\mathbf{U} &= \begin{bmatrix} \Delta\mathbf{u}(0)^\mathsf{T} & \Delta\mathbf{u}(1)^\mathsf{T} & \cdots & \Delta\mathbf{u}(N_o-1)^\mathsf{T} \end{bmatrix}^\mathsf{T} \\
\Delta\mathbf{D} &= \begin{bmatrix} \Delta\mathbf{d}(0)^\mathsf{T} & \Delta\mathbf{d}(1)^\mathsf{T} & \cdots & \Delta\mathbf{d}(N_p-1)^\mathsf{T} \end{bmatrix}^\mathsf{T}.
\end{aligned}$$

Assuming now availability of demand flow predictions at the origin links of the protected network over a prediction horizon N_p, i.e. $\Delta\mathbf{d}(k) \neq \mathbf{0}$, $k = 0, 1, \ldots, N_p - 1$, minimisation of the performance criterion (8) subject to (7) leads to the analytical solution:

$$\Delta\mathbf{U} = -\mathbf{H}^{-1}\mathbf{F}\big[\mathbf{x}(0) + \mathbf{G}\Delta\mathbf{D}\big], \tag{9}$$

where $\mathbf{H} = \mathbf{\Gamma}^\mathsf{T}\mathcal{Q}\mathbf{\Gamma} + \mathcal{R}$ is the Hessian of the corresponding quadratic program (QP), $\mathbf{F} = \mathbf{\Gamma}^\mathsf{T}\mathcal{Q}\mathbf{\Omega}$, and $\mathbf{G} = \mathbf{\Gamma}^\mathsf{T}\mathcal{Z}$. The matrices $\mathbf{\Gamma}$ and $\mathbf{\Omega}$ may be readily specified from the integration of (7) starting from the initial point $\mathbf{x}(0)$, while $\mathcal{Q}$, $\mathcal{R}$, $\mathcal{Z}$ are weighting matrices (in function of $\mathbf{Q}$, $\mathbf{R}$, and $\mathbf{C}$) over the optimisation N_o (see e.g. Goodwin et al. (2005) for details). Given that $\mathbf{R} \succ \mathbf{0}$ in the cost criterion (8) the Hessian $\mathbf{H}$ is positive definite, and thus the QP is convex and has a global optimum.

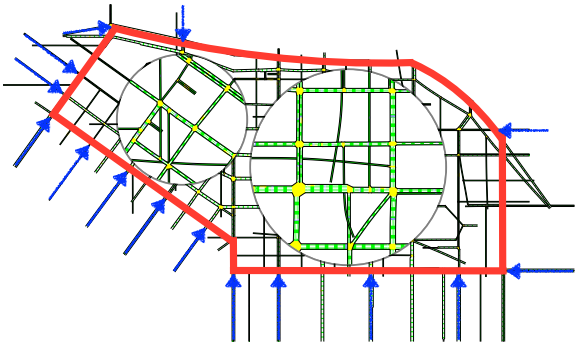

Figure 2: Protected network and controlled gates of entrance.

Using the above notation, we can express the problem of minimising (8) subject to the equality constraints (7) and inequality constraints (5)–(6) as follows:

$$\begin{aligned} &\min_{\mathbf{U}} \frac{1}{2}\mathbf{U}^{\mathsf{T}}\mathbf{H}\mathbf{U} + \mathbf{U}^{\mathsf{T}}\left[\mathbf{x}(0) - \mathbf{H}\hat{\mathbf{U}} + \mathbf{G}\Delta\mathbf{D}\right] \\ &\text{subject to:} \\ &\mathbf{L}\mathbf{U} \leq \mathbf{W} \end{aligned} \tag{10}$$

where $\mathbf{L}$ and $\mathbf{W}$ are matrices reflecting the lower and upper bounds of the state and control constraints (given state integration starting from the initial point $\mathbf{x}_0$) over the optimisation horizon N_o (see e.g. Goodwin et al. (2005) for details). Once the open-loop QP problem (10) is solved from the known initial $\mathbf{x}(0)$ and predicted disturbances $\mathbf{d}(k), k = 0, 1, \ldots, N_p - 1$, the rolling horizon scheme applies, at the current time k, only the first control move, formed by the first m components of the optimal vector $\mathbf{U}^*(\mathbf{x}_0)$ in (10). This yields a control law of the form

$$\mathbf{u}(k) = \mathcal{M}\left[\mathbf{x}(k), \mathbf{d}(\kappa)\right], \quad \kappa = k, k+1, \ldots, k+N_p-1 \tag{11}$$

where $\mathbf{x}(k) = \mathbf{x}_0$, $k = 0, \ldots, N_o - 1$ is the current state of the system and $\mathcal{M}$ is a linear mapping from the state and disturbance spaces to control. Then the whole procedure is repeated at the next time instant, with the optimisation horizon kept constant.

4 Case Study and Results

4.1 Case Study Description

Fig. 3 depicts the shape of O_c in function of $n(t)$ for the 2.5 square mile area of Downtown San Francisco, CA, including 110 junctions and 440 links (see Fig. 2). Fig. 3 confirms the existence of a fundamental diagram like-shape for the study area, which shape is seen to depend on the accumulation of vehicles. It can be seen that as the vehicle accumulation is increased from zero, the network flow increases to a maximum (flow capacity) and then turns down and decreases sharply to a low value possibly zero (in case of gridlock). Flow capacity (around $30 \cdot 10^4$ veh/h) is observed at a vehicle accumulation of about 6,000 veh. The shape of the fundamental diagram (and its critical parameters) was reproduced under different demand and OD scenarios with Dynamic Traffic Assignment activated to capture somewhat adaptive drivers in a microsimulation study via AIMSUN (Aboudolas and Geroliminis, 2013). The shape of O_c in Fig. 3 can be approximated by the following 3rd order polynomial:

$$O_c(n) = 4.128 \times 10^{-7} n^3 - 0.0136 n^2 + 113.264 n \tag{12}$$

where $n \in [0, 13000]$. To determine the output O from O_c an average trip length $L = 1.75$ km and average link length $l = 0.25$ km were considered. The value of L is consistent with the average trip length and the travel time across the test area of San Francisco.

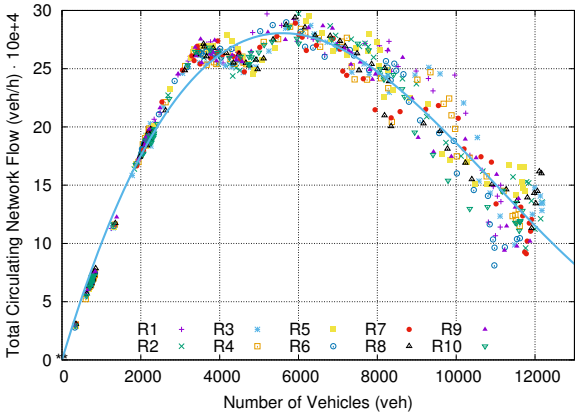

Figure 3: Network fundamental diagram of Downtown SF.

4.2 Controller Design

The desired vehicle accumulation for (7) is selected $\hat{n} = 4000$ veh, while $\hat{\ell}_o = 0, \forall o \in O$. Table 1 provides the different geometric characteristics of the fifteen ($|\mathcal{O}| = 15$) entrance links and controlled gates shown in Fig. 2 (illustrated with blue arrows). The third column provides the storage capacity of each controlled link that is the vector $\mathbf{x}_{\max}^{\mathsf{T}} = \begin{bmatrix} n_{\max} & \ell_{1,\max} & \cdots & \ell_{|\mathcal{O}|,\max} \end{bmatrix}$. The last three columns of the table provide the vectors $\mathbf{u}_{\min} = \mathbf{q}_{\min}$, $\hat{\mathbf{u}} = \hat{\mathbf{q}}$, and $\mathbf{u}_{\max} = \mathbf{q}_{\max}$, respectively. These values are calculated from the field applied signal plans presented in columns 5 (S_o: saturation flow), 6 (C: cycle length) , 7 ($g_{o,\min}$: minimum green time), 8 ($\hat{g}_o$: nominal green time), and 9 ($g_{o,\max}$: maximum green time), via gS/C. In this way, any input flows ordered by the distributed perimeter flow control strategy are feasible traffic signal plans. Note that traffic signals at controlled gates are all multiphase fixed-time operating on a common cycle length of 90 s for the west boundary of the area (gates $o = 1, \ldots, 11$) and 60 s for the rest (gates $o = 12, \ldots, 15$).

For the solution of (9) or (11) it suffices to specify the state matrices $\mathbf{A}$, $\mathbf{B}$, and $\mathbf{C}$, and weighting matrices $\mathbf{Q}$ and $\mathbf{R}$. All state matrices are constructed for the studied network on the basis of the selected $\hat{\mathbf{x}}^{\mathsf{T}} = [\hat{n} \quad \mathbf{0}]$, $\hat{\mathbf{u}} = \hat{\mathbf{q}}$ and $\hat{\mathbf{d}} = \mathbf{0}$, and sampling time $T = 180$ s. The matrix $\mathbf{Q} = \mathrm{diag}(1/w, 1/\ell_{1,\max}, \ldots, 1/\ell_{|\mathcal{O}|,\max})$ is selected, where $w = 2000$ veh was found appropriate to achieve equity. The diagonal elements of $\mathbf{R}$ were set equal to $r = 0.00001$. The disturbance vector $\mathbf{d}$ consists of the demands d_o, $o = 1, \ldots, 15$, at every origin of the protected network and disturbance d_n of the fundamental diagram. Trapezoidal demands have been used for $d_o(k)$, $o = 1, \ldots, 15$, $k = 0, \ldots, N_p - 1$ over a predicted horizon of $N_o = N_p = 40$. To capture the uncertainty of the (scaled) fundamental diagram, particularly when the network operating in the congested regime (notice the noise for $n > 6000$ veh), d_n is selected to vary gradually with respect to $n(k)$ in the range $[-3000, 3000]$ veh/h for $n > 6000$ veh.

Table 1: Different characteristics of entrance links and controlled gates.

Gate #	Length (m)	Capacity (veh)	No lanes	Saturation Flow (veh/h)	Cycle Length (s)	Min Green (s)	Nominal Green (s)	Max Green (s)	Min Flow (veh/h)	Nominal Flow (veh/h)	Max Flow (veh/h)
1	235	128	3	5400	60	15	33	39	1350	2970	3510
2	299	109	2	3600	60	12	30	42	720	1800	2520
3	299	163	3	5400	60	15	27	39	1350	2430	3510
4	271	98	2	3600	60	12	35	42	720	2100	2520
5	261	95	2	3600	60	12	24	42	720	1440	2520
6	299	109	2	3600	60	12	30	42	720	1800	2520
7	298	109	2	3600	60	12	36	39	720	2160	2340
8	298	109	2	3600	60	12	37	42	720	2220	2520
9	296	269	5	10000	60	17	27	31	2833	4500	5167
10	296	269	5	8800	60	16	27	38	2347	3960	5573
11	299	109	2	3600	60	12	25	42	720	1500	2520
12	190	103	3	5400	90	13	42	43	780	2520	2580
13	81	44	3	5400	90	12	18	41	720	1080	2460
14	81	44	3	5400	90	12	20	41	720	1200	2460
15	341	186	3	5400	90	12	48	59	720	2880	3540

4.3 Open-loop Control Results

Several tests were conducted in order to investigate the behaviour of the proposed distributed control for different scenarios. The scenarios were created by assuming more or less high initial queues $\ell_o(0)$ in the fifteen origin links of the protected network while the protected network area operating in the congested regime, i.e. its state $n(0) > 6000$ veh. The optimisation horizon for each scenario is 2 h (40 cycles).

Fig. 4 shows some obtained trajectories for a heavy scenario with $\ell_o(0) = 0.7\ell_{o,\max}, \forall o = 1, \ldots, 15$ and two initial states in the congested regime of the fundamental diagram $n(0) = 7000$ veh and $n(0) = 12000$ veh (extreme case). Tests were conducted with and without external demand flows at origin links, denoted with "s+d" and "s-d", respectively. It should be noted that despite the same level of saturation (70%) is used for all origin links, the corresponding vehicle queues observed vary due to different geometric characteristics. The main observations are summarised in the following remarks:

- The proposed strategy manages to stabilise the vehicle accumulation of the protected network around its desired point $\hat{n} = 4000$ veh for all initial points (even in the extreme case) and cases with and without disturbances (see Fig. 4(c)).
- The proposed distributed control strategy manages to dissolve the initial origin link queues in a balanced way (see Figs. 4(j–o)) and thus, the desired control objective of queue balancing and equity for drivers using different gates to enter the protected network area is achieved.
- The proposed strategy manages to stabilise all input flows to their desired values $\hat{\mathbf{q}}$ (corresponding to the nominal signal plan in Table 1) in the steady state, i.e., where $n = \hat{n} = 4000$ and system's throughput is maximised (see Figs. 4(d–i), notice the different reference points $\hat{q}_o$ in each subfigure).
- The input flows ordered by the distributed perimeter flow control strategy have different trajectories and characteristics (see control trajectories in Figs. 4(d–i)). This confirms that an equal distribution of ordered flows to corresponding junctions is not optimal, as largely assumed or ignored in previous studies. As can be seen, the proposed strategy determines optimally distributed input flows (or feasible entrance link green times) by taking into account the individual geometric characteristics of the origin links as well as minimum and maximum constraints.
- Excessive demand and high initial queues at origin links, coupled with the applied control, causes congestion shortly after the beginning of the time horizon. At the same time the protected network is operating in the congested regime ($n(0) = 7000$ veh or $n(0) = 12000$ veh). As can be seen, the distributed control strategy first restricts the high initial queues at origin links to flow into the oversaturated protected network area and then, in order to manage the developed long queues therein (in some cases reach the upper bounds), it gradually increases the input flows. Note that for some gates (7, 8 and 9) bound constraints are active for a certain time period.

Figs. 4(a, b) depict the state and control trajectories for the perimeter flow control problem without origin link dynamics, i.e. for the single-input single output control problem with only (1). For this problem $\hat{n} = 6000$ veh is considered. As can be seen, the strategy manages to stabilise the vehicle accumulation of the protected network around its desired point $\hat{n} = 6000$ veh starting from a number of different initial points. The strategy restricts flow to enter the protected network area whenever $n > 6000$, while increases the input flows for $n < 6000$. It is evident that the single-region control strategy without queue dynamics outside of the protected area needs more time and effort to stabilise the system at $k = 60$, compared to the proposed distributed perimeter flow control, which stabilises all queues and protected network's accumulation at $k = 40$. This is attributed to the complete lack of information of the geometric characteristics of the origin links that affects control decisions. On the other hand, the control flexibility and efficiency of the proposed control while explicitly considering the queue dynamics and constraints underlines the clear superiority of appropriate distributed flow control.

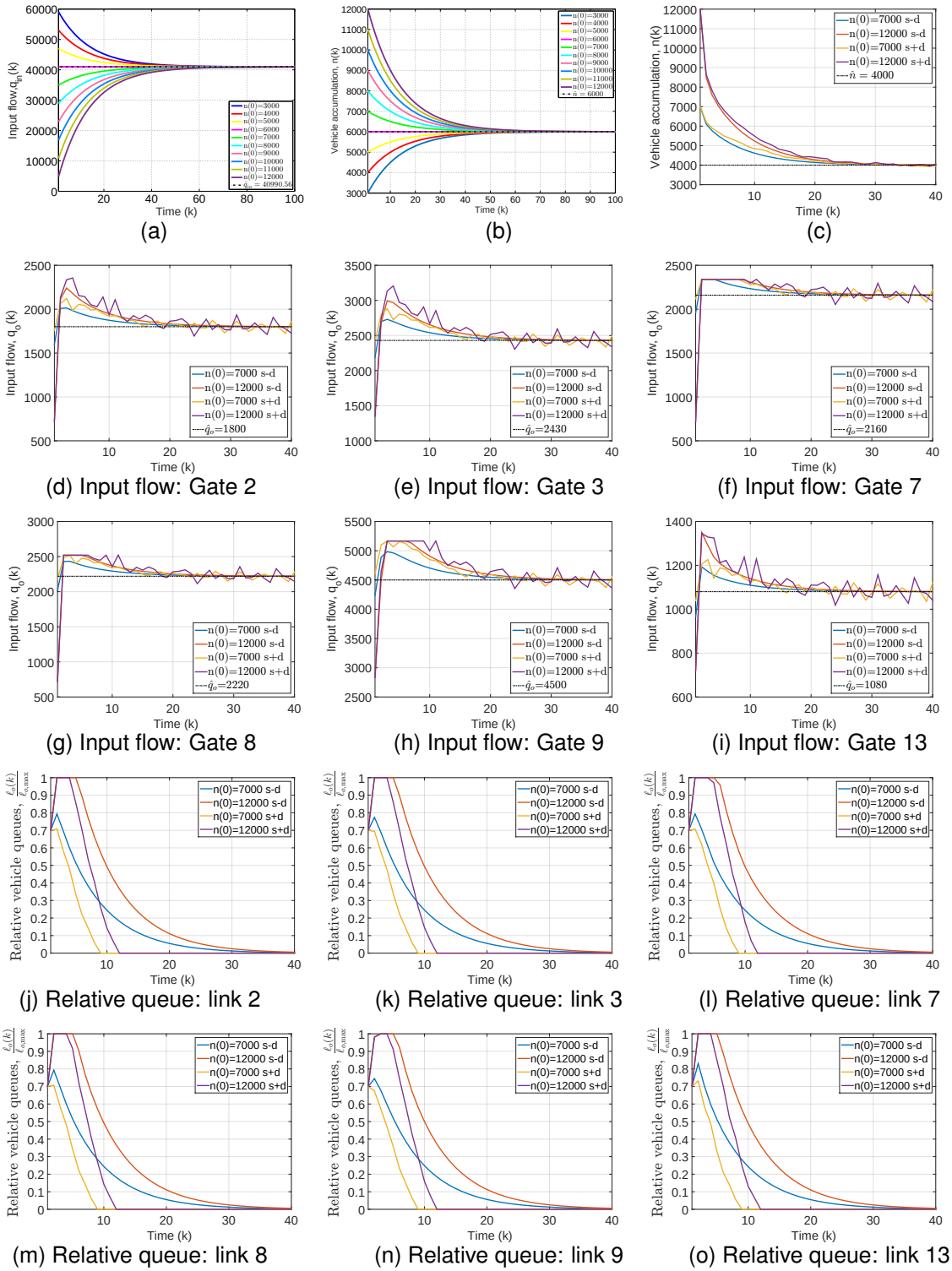

Figure 4: (a, b) State and control trajectories without link dynamics; (c) State trajectories of the protected network for different initial points with and without disturbance; (d–o) State and control trajectories of six selected origin links (gates) for different initial points with and without disturbance.

5 Conclusions

In this paper, an integrated model for distributed perimeter flow control is presented. Compared to previous works, the proposed scheme determines optimally distributed input flows for a number of gates located at the periphery of a protected network area. Simulation results for a protected area of downtown San Francisco with fifteen gates of different geometric characteristics were presented. Results demonstrated the efficiency and equity properties of the proposed approach to better manage excessive queues outside of the protected network area and optimally distribute the input flows. It is expected that similar policies can also be utilised for dynamic road pricing. Future research will focus on the efficiency versus equity properties of perimeter flow control with queue dynamics and the integration of additional components for dynamic road pricing.

References

Aboudolas, K., Geroliminis, N., 2013. Perimeter and boundary flow control in multi-reservoir heterogeneous networks. Transportation Research Part B 55, 265–281.

Ampountolas, K., Kouvelas, A., 2015. Real-time estimation of critical vehicle accumulation for maximum network throughput. In: 2015 American Control Conference (ACC). pp. 2057–2062.

Ardekani, S., Herman, R., 1987. Urban network-wide traffic variables and their relations. Transportation Science 21 (1), 1–16.

Csikós, A., Tettamanti, T., Varga, I., 2015. Nonlinear gating control for urban road traffic network using the network fundamental diagram. Journal of Advanced Transportation 49 (5), 597–615.

Daganzo, C. F., 2007. Urban gridlock: Macroscopic modeling and mitigation approaches. Transportation Research Part B 41 (1), 49–62.

Daganzo, C. F., Geroliminis, N., 2008. An analytical approximation for the macroscopic fundamental diagram of urban traffic. Transportation Research Part B 42 (9), 771–781.

Farhi, N., Goursat, M., Quadrat, J.-P., 2011. The traffic phases of road networks. Transportation Research Part C 19 (1), 85–102.

Geroliminis, N., Daganzo, C. F., 2008. Existence of urban-scale macroscopic fundamental diagrams: Some experimental findings. Transportation Research Part B 42 (9), 759–770.

Geroliminis, N., Haddad, J., Ramezani, M., 2013. Optimal perimeter control for two urban regions with macroscopic fundamental diagrams: A model predictive approach. IEEE Transactions on Intelligent Transportation Systems 14 (1), 348–359.

Godfrey, J. W., 1969. The mechanism of a road network. Traffic Engineering and Control 11 (7), 323–327.

Goodwin, G., Seron, M. M., de Don, J. A., 2005. Constrained Control and Estimation: An Optimisation Approach. Springer-Verlag, London, UK.

Haddad, J., 2015. Robust constrained control of uncertain macroscopic fundamental diagram networks. Transportation Research Part C 59, 323–339.

Herman, R., Prigogine, I., 1979. A two-fluid approach to town traffic. Science 204, 148–151.

Keyvan-Ekbatani, M., Kouvelas, A., Papamichail, I., Papageorgiou, M., 2012. Exploiting the fundamental diagram of urban networks for feedback-based gating. Transportation Research Part B 46 (10), 1393–1403.

Mahmassani, H., Williams, J., Herman, R., 1987. Performance of urban traffic networks. In: Gartner, N., Wilson, N. (Eds.), 10th International Symposium on Transportation and Traffic Theory. Elsevier, Amsterdam, The Netherlands.